

Poly(o-aminophenol) Electrosynthesized onto Platinum at Acidic and Neutral pH: Comparative Investigation on the Polymers Characteristics and on Their Inner and Outer Interfaces

M. E. Carbone, R. Ciriello, A. Guerrieri, A. M. Salvi*

Department of Science, DiS, University of Basilicata Viale dell'Ateneo Lucano, 10 - 85100 Potenza, Italy

*E-mail: anna.salvi@unibas.it

Received: 20 November 2013 / Accepted: 13 December 2013 / Published: 2 February 2014

The polymer formed by electrochemical oxidation of o-aminophenol (oAP) on platinum substrates, both in neutral and acidic media, has been characterized. Attention was focussed on the three constituent phases: the polymer itself and its inner (metal/polymer) and outer (polymer/electrolytic solution) interfaces. As well known, poly(o-aminophenol) (PoAP) consistently shows tuneable properties depending on pH, evidencing a remarkable electroactivity or a strong passivating behaviour if synthesized in acidic and in neutral/basic media, respectively. Although much investigated, a full understanding of the polymerization routes has not yet been reached for either the conducting and insulating films. To improve this situation studies on PoAP were conducted with a combination of techniques: Cyclic Voltammetry (CV); X-ray Photoelectron Spectroscopy (XPS); Atomic Force Microscopy (AFM); and micro-Raman. It was thus possible to compare compositional and morphological analyses, highlighting in turn different analytical depths of our PoAP/Pt systems. The results here obtained add new information on how to recognize the influence of platinum oxidation and its cleanliness on interface reactions. It was also found that, in order to estimate properly the real structure of both insulating and conducting PoAP, the presence of oxidized terminal groups and water molecules strongly bonded along the polymer chains must be taken into account.

Keywords: Poly(o-aminophenol)/Pt, CV, XPS, AFM, Micro-Raman

1. INTRODUCTION

Organic films electrodeposited on metallic surfaces have revealed interesting properties depending on chemical composition and morphology, growth conditions and electrochemical

environments [1]. They have shown to be of great utility in many areas of research, for example, as basic components in electrocatalysis, biosensor and electrochromic devices and as protective agents against corrosion [2]. In the last few decades attention was focused on organic films made of aromatic compounds such as phenols, anilines and, more recently, aminophenols, interesting members of the class of substituted anilines. Within the various isomers, oAP has attracted most attention because of its ability to form conductive or insulating polymers (PoAP) under electrochemical oxidation in acidic and neutral/basic media, respectively [3,4].

As derived from literature data specifically devoted to PoAP, recently reviewed [5-7], hypotheses on the polymerization mechanisms are derived from studies performed with various means of investigation, electro-synthesis conditions and electrode types. They all converge on identifying the phenoxazine units as the main component of a 'ladder' conducting PoAP and the azo-compound 2,2'-dihydroxyazobenzene, DHAD, as the main dimerization product for insulating PoAP.

However, controversies are also reported regarding the identification of possible intermediates leading to side reactions, facilitated by the simultaneous presence on oAP of hydroxide and amine groups, both prone to oxidation. The comprehension of the real structure of both conducting and insulating PoAP film is therefore hindered.

In this work, to gain a further insight into the polymerization routes of PoAP, and to identify similarities and differences in its conducting and insulating state, we have performed the same investigation on both kind of polymers using XPS in combination with micro-Raman thus highlighting different sampling areas and depths, according to the specificity of each technique. Notably, the analytical capability of XPS has allowed a step forwards by providing, through curve-fitting [8], a reproducible semi-quantitative analysis of both films, within the outer layers, at the nanometers scale.

Moreover, by combining CV, XPS and AFM analyses, we have examined the surface state of platinum used as working electrode and varied, as appropriate, its degree of oxidation to monitor the effect of the normally adopted cleaning procedures and the role of pre-adsorbed oxygen on the first adhesion and subsequent film growth [9,10] for both PoAP electro-synthesis procedures.

The results obtained are discussed by referring, whenever appropriate, to specific articles that relate to our experimental conditions, among those cited in the reported reviews.

2. EXPERIMENTAL

2.1 Materials

Ortho-aminophenol (oAP) was obtained from Sigma Aldrich (Germany) and purified by recrystallization in ethyl acetate [11]. All other chemicals were of analytical grade and were used without further purification. Care was taken to prepare the solutions immediately before use in ultra pure water, filtered through a combined Elix-5/Milli-Q (Millipore, Milan S.p.A.) system.

2.2 Electrochemical apparatus

Electrochemical experiments were carried out with an EG&G PAR model 263A potentiostat/galvanostat. Data acquisition and potentiostat control were accomplished with a desktop computer running the M270 Electrochemical Research Software (EG&G), version 4.23. The electrochemical cell was a conventional three-electrode system with a Pt counter electrode, an Ag/AgCl, KCl sat. reference electrode and the working electrode consisted of platinum foil (10x15x0.127mm).

2.3 Platinum cleaning procedure

Platinum working electrodes were initially cleaned following the procedure elsewhere reported [12]: (1) chemically treated with hot concentrated (70%) HNO₃ in an ultrasonic bath for few minutes; thoroughly rinsed with water to remove any residual HNO₃; (2) mechanically rubbed with alumina 0.05 μm, using a polishing cloth; sonicated in water for several minutes to remove any Al₂O₃ residue from the surface; (3) activated by CV in 0.5 M H₂SO₄, scanning 20 cycles in the potential range of -0.225 / +1.225 V vs Ag/AgCl at a scan rate of 100 mV/s.

During the course of this investigation, the procedure was modified by reversing the order of the chemical etching and the mechanical cleaning steps (see section 3.3).

2.4 Electrochemical synthesis of PoAP

PoAP films were electrochemically grown on platinum foils by cyclic voltammetry. The conducting polymer was normally prepared by 125 scan cycles using a 5 mM oAP solution in perchlorate electrolyte (HClO₄/KClO₄, 0.1 M, pH 1). The potential ranged from -0.2 to +0.9 V (vs. Ag/AgCl, saturated KCl) at a scan rate of 50 mV/s. The deposited film appears as a brown adherent coating on the platinum substrate.

The insulating, transparent, polymer was electrosynthesized by scanning the electrode potential for 20 cycles between -0.1 and +0.9 V (vs. Ag/AgCl, saturated KCl) in a 5 mM oAP solution in a phosphate buffer (I=0.1 M, pH 7) at a scan rate of 50 mV/s.

Electrochemically synthesized PoAP films were then washed with double-distilled water and dried at room temperature in nitrogen atmosphere before their ex-situ analyses.

2.5 XPS

The XPS spectra of the monomer, oAP, were acquired with a LH X1 Leybold instrument using the achromatic Al Kα (1486.6 eV) source operating at a constant power of 260 W. Under these conditions, the instrumental contribution to line-width is kept constant and the measured FWHMs (Full Width Half Maximum) of Au 4f_{7/2} (84.0 eV) and Cu2p_{3/2} (932.7 eV) signals used for calibration purposes were 1.3 and 1.6 eV, respectively. Powdered samples of purified oAP were mounted as a

pellet on a heatable/coolable sample probe using double-sided copper adhesive tape. To avoid any sample sublimation into the analysis chamber under the ultra-high vacuum conditions (UHV), the sample probe was cooled with liquid nitrogen prior to, and during, XPS analysis. Wide and detailed spectra were collected using the FAT (fixed analyzer transmission) mode of operation with a pass energy of 50 eV and a channel width of 1.0 and 0.1 eV, respectively.

XPS analysis of the electrochemically treated platinum foils was performed by a Phoibos 100-MCD5 spectrometer, operating in Medium Area lens mode (spot of $\varnothing = 2$ mm, entrance slit of 7x20 mm) to selectively analyze blank and deposited zones (vide infra). Spectra were acquired with achromatic Al K α radiation (1486.6 eV) operating at 10 kV and 10 mA. The pressure in the analysis chamber was typically about 10^{-9} mbar during acquisition. To give the same spectra resolution as that obtained with the Leybold spectrometer a pass energy of 9 eV was used to collect the wide and the detailed spectra, again using fixed analyzer transmission (FAT) operation mode with channel widths of 1.0 and 0.1 eV, respectively.

All XP spectra were acquired at a 90° takeoff angle. The energy scale of the spectrometer was calibrated with Cu2p_{3/2} (932,7 eV) and Au4f_{7/2} (84,0 eV) signals using pure metals (Johnson Matthey) for spectroscopic analysis.

2.5.1 Curve-Fitting Procedure

The XPS spectra acquired from both spectrometers were analyzed using a curve-fitting program Googly which gives to each individual peak its own intrinsic Shirley-like background [13] and extrinsic tail, as fully described in previous works [8,14]. Peak areas were converted to atomic composition using established procedures and the appropriate sensitivity factors, SF [15]. The criteria adopted for data elaboration were based on preliminary analyses of reference compounds and literature data to assure the correct elemental mass balance, in the limit of our accuracy [16,17]. The XPS figures reported in this paper are not corrected for surface charging but the peak assignments (Binding Energies, BEs), as reported in Table 1, are referenced to C1s aromatic carbon, as an internal standard, set at 284.8 eV.

Table 1. Curve-fitting parameters of detailed regions shown in Figure 1.

Element	Peak number	BE corr. (ev)	FWHM (eV)	Corrected area (arbitrary units)	Assignment
C1s	0	283.0	1.77	713.39	Contam.
	1	284.8	1.92	16014.66	C _{arom.}
	2	285.3	1.92	4562.58	C-NH ₂
	3	286.4	1.72	4562.58	C-OH
	4	290.9	2.14	889.70	Shake up
	5	292.5	2.14	889.70	Shake up
O1s	0	530.5	2.25	157.71	Contam.
	1	533.1	2.25	5312.69	C-OH + H ₂ O
	2	539.6	2.03	193.38	Shake up
N1s	1	399.9	1.95	4445.92	C-NH ₂
	2	406.3	1.38	117.41	Shake up

The wide spectra are reported, as acquired, in kinetic energy, whereas the energy scales of the detailed regions are converted to binding energy so as to facilitate comparison of the curve fitted results with literature data.

2.6 Micro-Raman spectroscopy

Raman spectra were recorded in backscattered configuration using a Horiba Jobin-Yvon LABRAM HR 800 micro-Raman spectrometer, equipped with two holographic gratings (600 grooves/mm and 1800 grooves/mm) and with an Olympus microscope supplied with 10x, 50x and 100x objectives. The spectrometer was connected to a CCD detector. Excitations were performed by 632.8 nm radiation from a He-Ne laser source. The laser power was set at about 8 mW by using an optical density filter. The spectra were acquired using the 600 grooves/mm grating and the 100x objective. In these conditions, the estimated resolution was around 4 cm^{-1} . The measurement times were in the 30–60 s range.

2.7 AFM analysis

AFM images were carried out by using the XE-120 microscope (Park Systems) in air and at room temperature. Data acquisition was carried out in non contact mode at scan rates between 0.15 and 2.20 Hz, using ultrasharp rectangular Si cantilevers (NCHR, Park Systems, tip radius less than 5 nm) with the nominal resonance frequency and force constant of 330 kHz and 42 N/m, respectively.

3. RESULTS AND DISCUSSION

3.1 XPS analysis of the monomer, oAP

As a first step of this research we have analyzed by XPS the reagent monomer (oAP) after purification. Figure 1A shows the wide spectrum of oAP, acquired with achromatic AlK α source, with labelled XPS and Auger peaks. The detailed C1s, O1s, N1s regions, acquired at higher resolution, are reported in Figure 1B with the component peaks resolved by curve-fitting. For each curve-fitted region, the component peaks are numbered and identified in Table 1 in terms of corrected BE, FWHM, normalized areas and chemical state assignment based on literature data [16-18].

Shake up peaks (due to $\pi \rightarrow \pi^*$ transitions) are evidenced on the high binding energy side of each region, as expected for aromatic compounds [19-21], ranging in intensity within a few % of that of the parent peak. The most intense satellites, split in two contributions, are seen in the carbon region. On the lower energy side of both carbon and oxygen regions, small peaks are present, labelled “peak 0”, and identified as contaminants probably deriving by condensation of carbon and oxygen containing species on the outer surface of the sample under cooling during XPS acquisition. By adding the intensity of shake-up satellites to that of the parent peaks [16,17] and neglecting “peaks 0” as

contaminants unrelated to the monomer, the XPS results are quite straightforward and in agreement with the elemental composition of oAP.

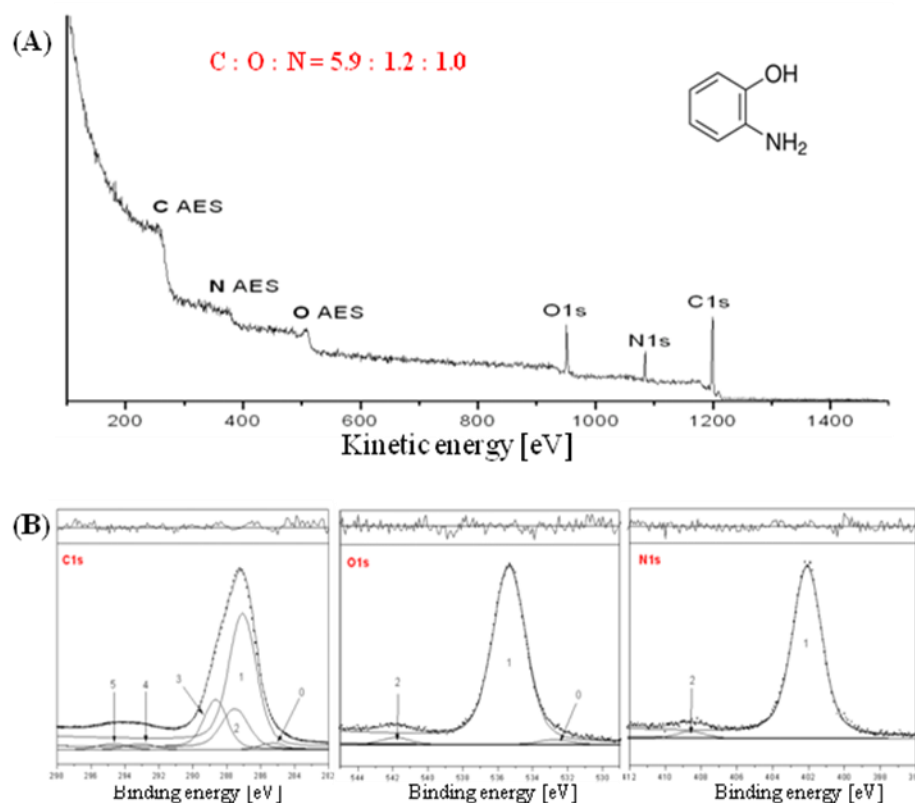


Figure 1. XPS analysis of ortho-aminophenol (oAP). (A) Wide spectrum and (B) C1s, O1s and N1s curve-fitted regions.

N1s shows only one component centred at 399.9 eV, a binding energy typical of C-N groups [22,1], plus its shake up satellite at 6.4 eV higher BE.

O1s also shows only one component (excluding “peak 0”) centred at 533.1 eV, typical of phenolic/ether oxygen [18,21] plus its shake up satellite shifted 6.5 eV, similarly to nitrogen.

C1s shows three components (again excluding “peak 0”). The first one set at 284.8 eV, the binding energy of aromatic carbon [18-23], plus two shake up satellites resolved by curve-fitting at 6.1 eV and 7.7 eV, higher BE. The second and third peaks, set at 285.3 eV and 286.4 eV, shortly separated, were resolved by curve-fitting using slightly different FWHMs to achieve the expected 1:1 area ratio, represent $\underline{\text{C}}\text{-N}$ and $\underline{\text{C}}\text{-O}$ groups, on the basis of the oAP chemical formula (see Figure 1 inset).

By comparing the intensities of the peaks (normalized areas) in Table 1, we see that the theoretical mass balance is always respected, within the limits of XPS accuracy [16,17], with the exception of the O1s area, resulting in excess oxygen, either in the partial or total cross-checking. The total C: O: N ratio is found to be 5.9:1.2:1 very close to that expected 6:1:1 with just the oxygen intensity beyond the upper limit ($\pm 10\%$) of the error interval associated with quantification.

An explanation for the oxygen in excess could be found in water vapour being condensed on the monomer surface as for the volatile organic contaminants, “peaks 0”. The only peculiarity, in this case, is that oxygen of condensed water shows the same binding energy of phenolic oxygen expressed by O1s peak 1 maximum at 533.1 eV and thus difficult to resolve by curve-fitting.

We will refer to XPS spectrum taken for oAP as a reference spectrum and the results shown in Figure 1 and Table 1 will be taken as a guidance for interpreting XPS spectra of the polymers, PoAP. As will be shown in the next paragraphs, the possible overlapping in energy between water and phenolic/ether oxygen is worth considering.

3.2. Characterization of the platinum surface and deposited ‘insulating’ PoAP

As a second experimental phase we examined the platinum surface state and its eventual influence on the first interfacial reactions occurring at the electrode surface that lead to film deposition and growth. CV, XPS and AFM were used to examine two differently treated platinum surfaces either before or after deposition of insulating PoAP. Making use of its inherent thinness [6] we expected to obtain evidence in the spectra of the underlying platinum.

3.2.1 CV analysis

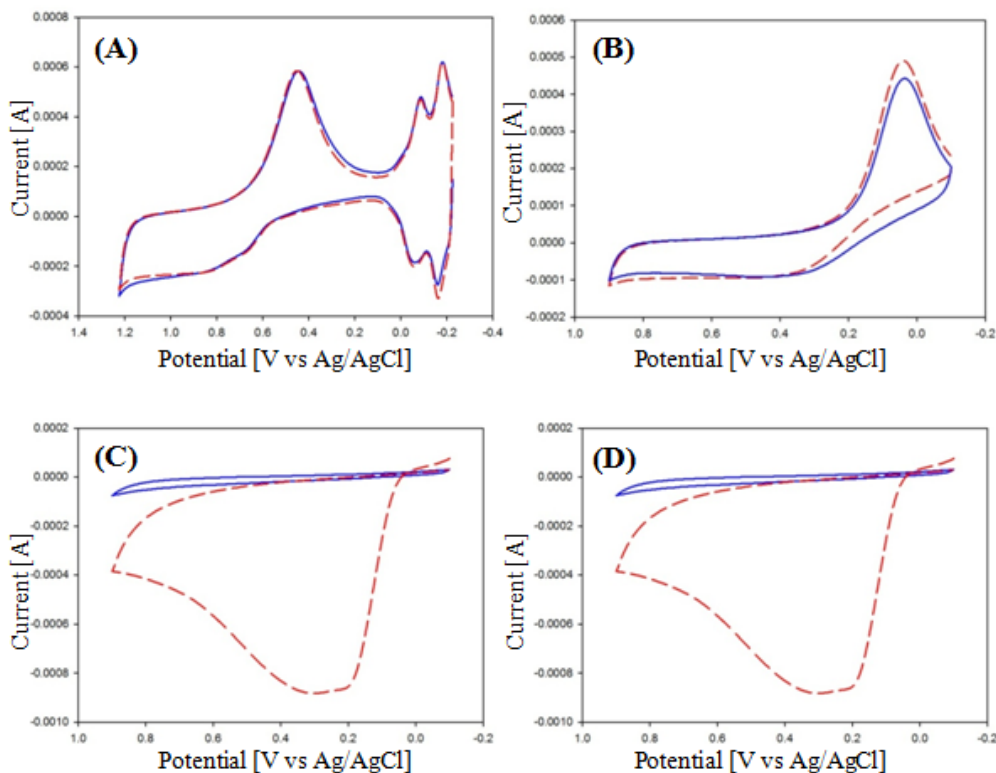


Figure 2. Cyclic voltammograms (1st (---) and 20th (—) scan) of (A) Pt foil in H₂SO₄ 0.5 M, blank 1; (B) (A) further cycled in phosphate buffer (pH=7, I=0.1 M), blank 2; PoAP electro-synthesized in 5 mM oAP/phosphate buffer solution onto (C) blank 1 and (D) blank 2 substrates; scan rate: 50 mV/s.

In Figures 2A-D are reported the relevant cyclic voltammograms. Particularly, Figure 2A shows the CV of a platinum foil activated in H₂SO₄ (0.5 M) following the pre-cleaning procedures listed in Experimental (blank 1), whereas Figure 2B shows the CV of the same platinum foil treated as in 2A and further cycled in the same neutral medium (phosphate buffer) used for oAP polymerization, applying the same potential interval (-0.1 / +0.9V vs Ag/AgCl) and number of scans (20 cycles), i.e. exactly the same conditions used for polymerization but in the absence of oAP (blank 2). Comparing the CVs, platinum signals are seen to shift towards less anodic potentials by passing from acidic (2A) to neutral (2B) media suggesting a favoured tendency of platinum to oxidize. Both blanks were obtained by ‘fully’ immersing the platinum foil into the electrolyte solutions (leaving just out the upper zone where electrical contacts for the electrochemical cell are set). Subsequently, after rinsing with bi-distilled Milli-Q water, only half of the blank electrodes was re-immersed in the monomer solution (oAP 5 mM, phosphate buffer, pH=7) for the PoAP electro-deposition. In this way, two well separated zones were available for the subsequent ex situ analyses of the treated platinum foils: the blank and deposited zones.

In Figure(s) 2C-D are reported CVs showing the first and the last 20th cycle, sufficient to achieve the complete electrode passivation, of the insulating PoAP electro-synthesized on platinum substrates blank 1 and blank 2, respectively. As previously reported [24], most of the polymerization process occurs in the first cycle. It can be seen that no significant differences appear in the polymerization profiles of Figures 2C-D.

3.2.2 XPS study

In Figures 3 and 4 are reported XPS spectra of the electrochemically treated platinum foils, rinsed with Milli-Q water and dried with gaseous nitrogen before insertion in the spectrometer. Using the Phoibos Medium Area modality, assisted by the laser-pointing/video camera system, the blank and deposited zones, as indicated in Figures 2, could be separately acquired. For each figure, the wide spectrum, insets of the detailed regions of interest and the overall atomic areas ratio are reported. Concerning the blank substrates (3A-B), evidence for the expected differences due to their diverse initial surface state can be seen by comparing their spectra and the relative carbon and oxygen intensities referenced to platinum (see figure insets), indicating a higher degree of oxidation for the substrate cycled in buffer phosphate.

It should be said that our experiments are not performed under ‘controlled’ atmosphere: we use, for example, ‘aerated’ electrochemical solutions and samples are stored in plugged vials filled with nitrogen for ex-situ transfers. Surfaces may therefore show slightly variable states if procedures and times are not accurately controlled. XPS repeats have proved the degree of oxidation and further adsorption of carbon-containing contaminants to be also dependent on the residence time of the substrates in the spectrometers.

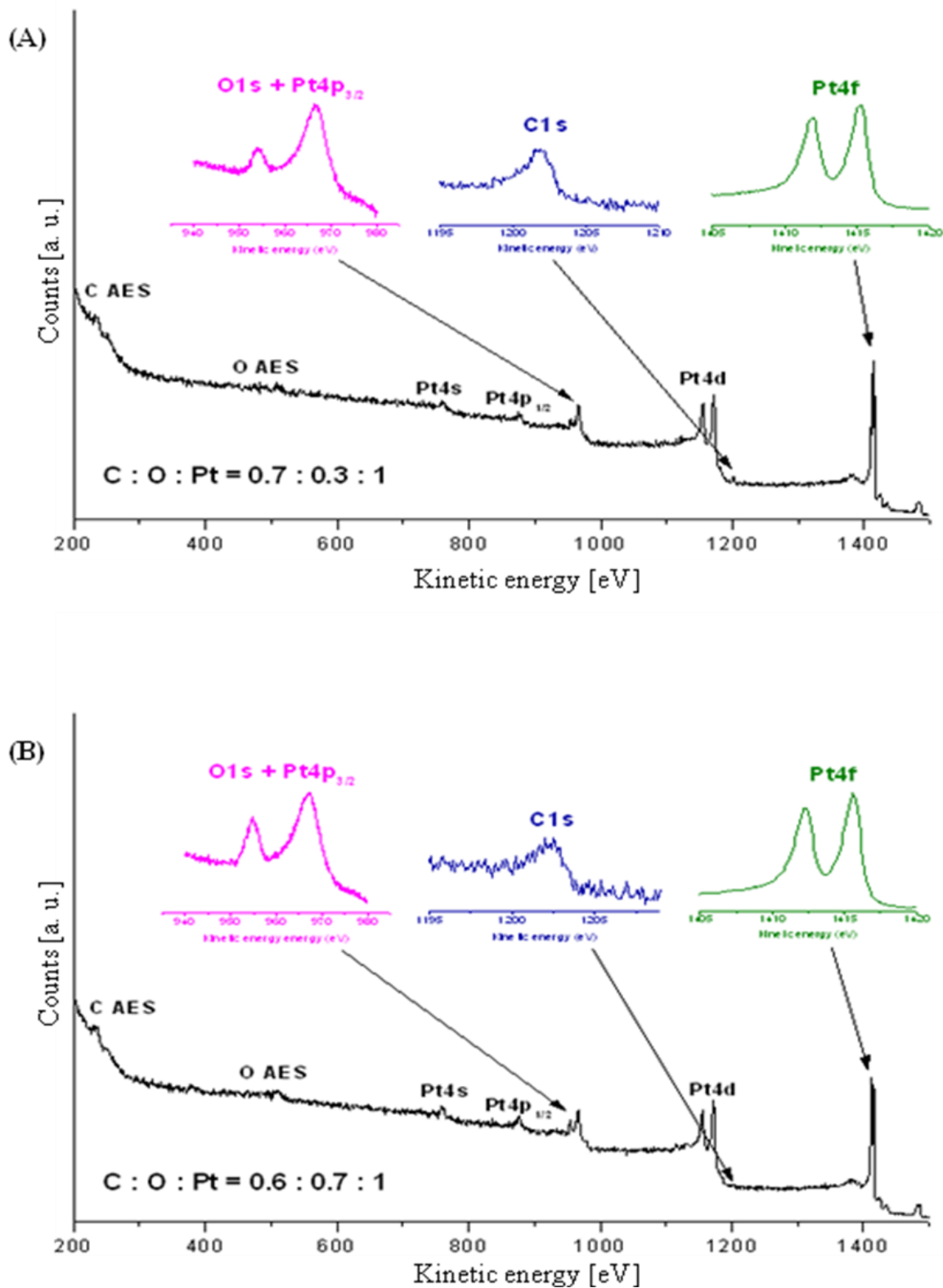


Figure 3. XPS wide spectra of (A) Pt foil cycled in H_2SO_4 0.5 M, blank 1; (B) (A) further cycled in phosphate buffer (pH=7, I=0.1 M) solution, blank 2. The insets show the corresponding O1s+Pt4p_{3/2}, C1s and Pt4f detailed regions.

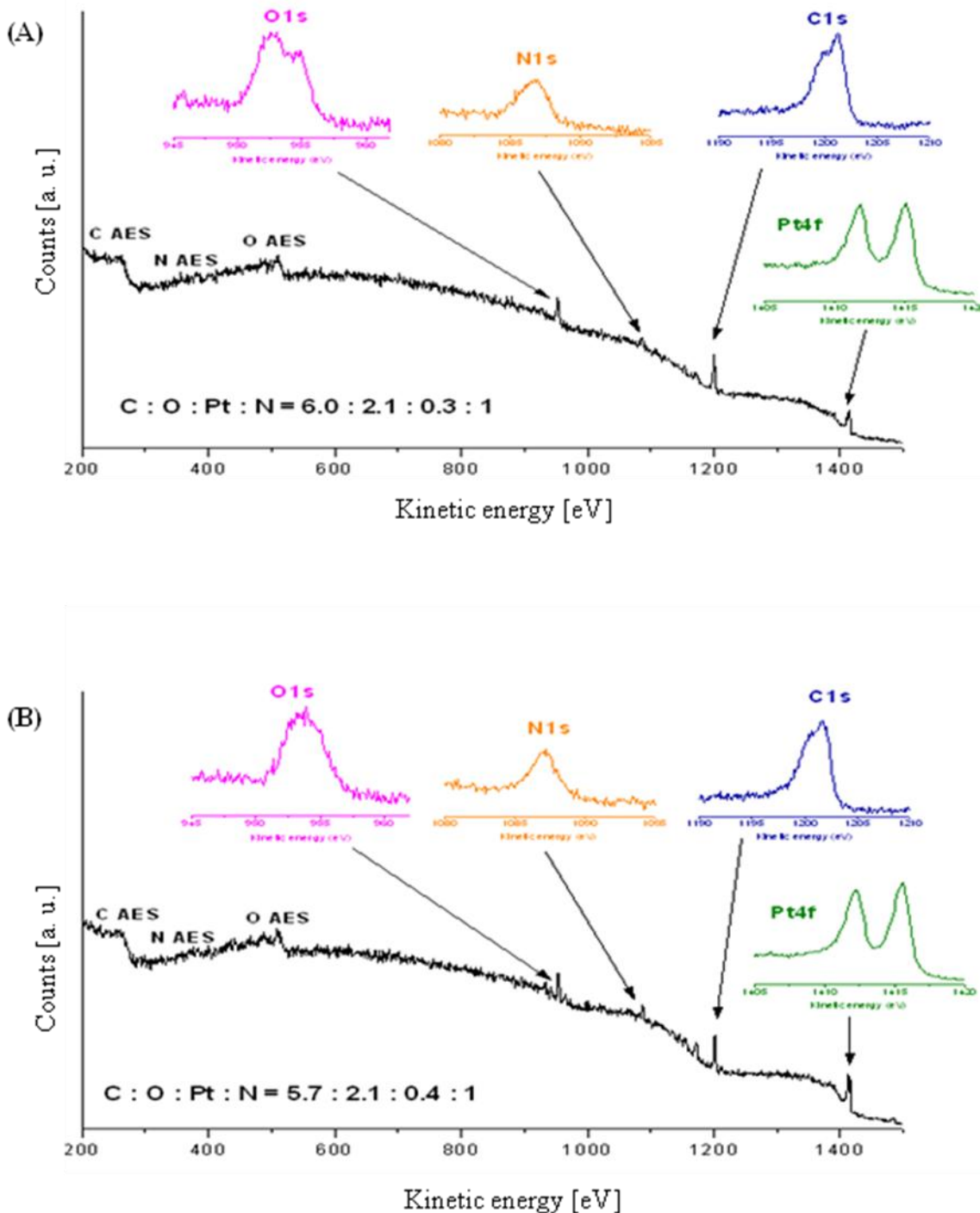


Figure 4. XPS wide spectra of insulating PoAP films electrosynthesized according to the conditions reported in Fig. 2C and 2D. The insets show the corresponding C1s, O1s, N1s and Pt4f detailed regions.

However, the two situations here represented were reproducibly obtained and were therefore analyzed to reveal the effect of substrate surface state on PoAP electro-deposition. To this aim, we based our assumptions on the reported correlation between oxygen coverage (in form of hydroxides for

experimental conditions similar to ours) and electrochemical oxidation of platinum at different potentials and time. The oxygen coverage can be derived from the XPS corrected O/Pt intensities [25]. In our case, more than a complete monolayer of adsorbed hydroxides together with platinum coordinated with further adsorbed hydroxides are likely to be formed on the surfaces of blank 1 and blank 2, respectively.

Regarding the insulating films (4A-B), differences in their spectral shapes and atomic ratios are again not significant, as found for their CVs. Moreover, they both show an amount of oxygen, in their C:O:N area ratio, double than that expected (6:1:1) by considering the repetition of the starting monomer, oAP, in the polymerization process. Importantly, the oxygen 1s clearly shows two components at around 531.5 eV (O1) and 533.2 eV (O2) having a O1:O2 ratio of about 0.8 for both films, irrespectively of the blank substrate on which they are deposited. Carbonyls groups and platinum hydroxide could both contribute to O1 [18, 21, 25, 26] while O2 has maintained the same BE of phenolic/ether oxygen but there, as seen from XPS of the monomer, strongly adsorbed water can contribute too.

3.2.3 Morphological investigation by AFM

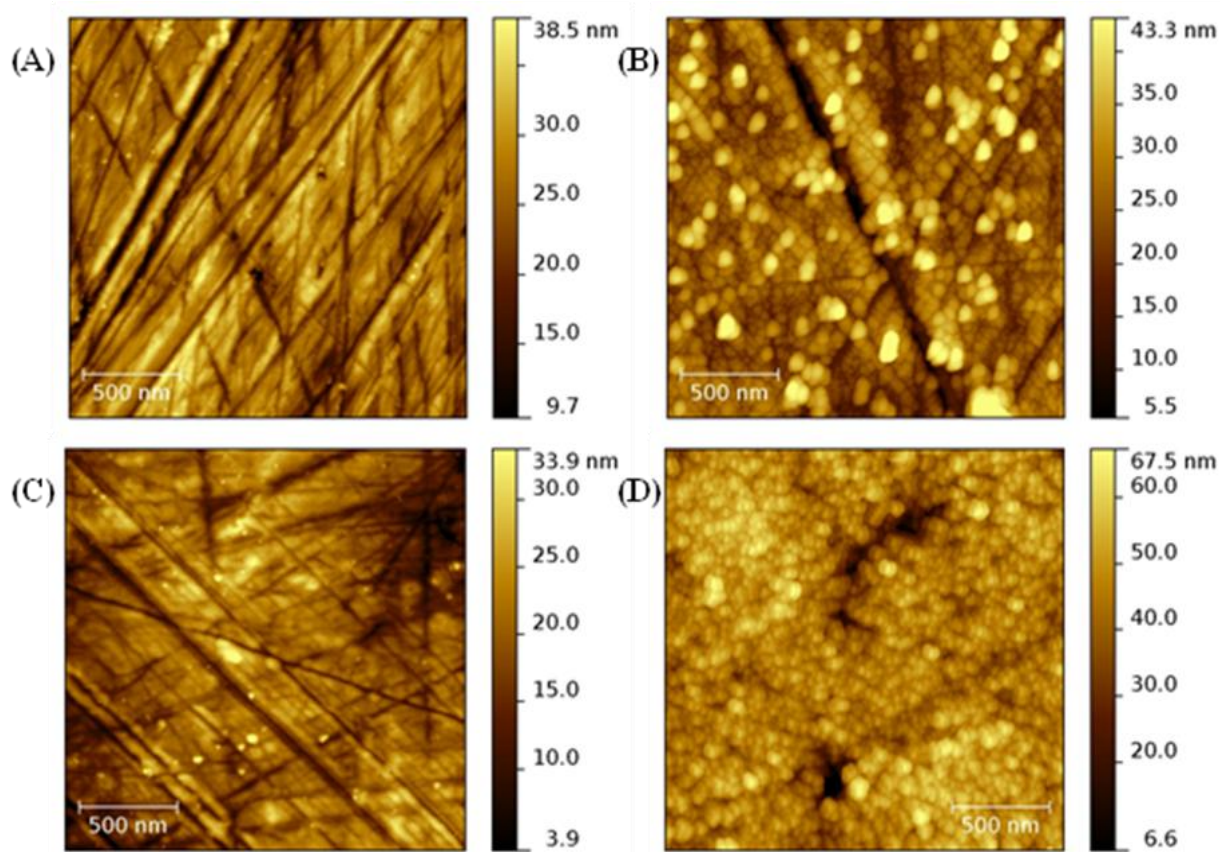


Figure 5. AFM images of (A) Pt foil cycled in H_2SO_4 0.5 M, blank 1; (B) (A) further cycled in phosphate buffer (pH=7, I=0.1 M) solution, blank 2; PoAP films electro-synthesized onto blank 1 (C) and blank 2 (D) substrates.

In Figures 5A-D are reported the AFM images of the same sample's sequence as reported in the previous figures in order to add information on substrate surface (topography) and film morphology.

At wide fields of view, it is difficult to discern blank and deposited zones for both platinum foils. This means that oAP film grows by 'retracing' the features of the underlying platinum. Another similarity of both sets is the presence of aggregates irregularly protruding all over the polymer zone. By gradually increasing the magnification, the different morphologies are made clearer and the pictures selected in Figures 5 are those magnified at the best resolution attainable.

The images of deposited zones (5C-D) show the film grown on blank 1 substrate (5C) smoother and more homogeneous and the film grown on blank 2 substrate (5D) having a granular aspect and irregular growth. By comparing the images of correspondent blank substrates (5A-B), it is easily derived that each film has grown by mirroring the initial substrate morphology and that insulating PoAP with the required smoothness and compactness can only be formed on less oxidized platinum surfaces, of about one monolayer coverage, as for blank 1 (5A).

On one hand, the two deposits strongly differ in their morphology depending on the surface state of the substrate on which they are deposited but on the other hand they look very similar both from the spectroscopic and electrochemical points of view. This confirms, what has been already reported [2, 9, 27] for other studies on the reactivity of Pt surfaces, that pre-existing oxygen can be displaced during oAP adsorption. Over a certain amount of oxygen, the displacement can be difficult and influence the kinetics of the polymerization process and subsequent organization of the polymer chains as well as the permeability and wettability of the finite PoAP.

3.3 CV, XPS and AFM analyses of conducting PoAP deposited on platinum

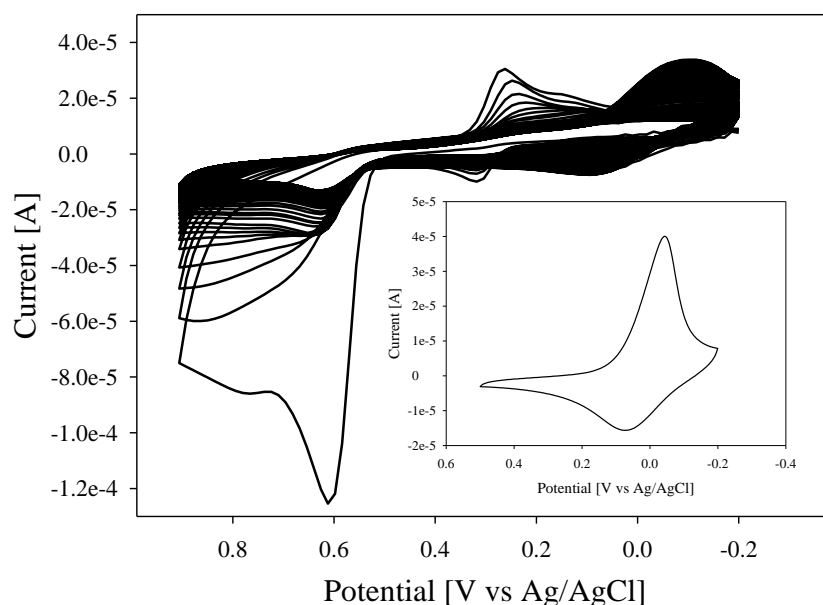


Figure 6. Voltammetric profiles acquired during the PoAP electro-synthesis (up to 125 cycles) onto a blank 1 Pt foil in a 5 mM oAP/perchlorate buffer solution (HClO_4 , KClO_4 0.1 M, $\text{pH}=1$). The inset shows the cyclic voltammogram of the deposited film in the same electrolyte without the monomer. Scan rate: 50 mV/s.

Based on previous results, the platinum electrode to be used for the deposition of conducting PoAP was cleaned as for blank 1, see Experimental, avoiding further activation in the same electrochemical solutions used for the electro-synthesis, in this case perchlorate electrolyte, pH=1. Figure 6 shows the CV acquisitions of conducting PoAP (5 mM oAP in 0.1 M HClO₄/KClO₄). The voltammetric profiles of the first 125 growth cycles, there reported, are those expected on the basis of literature data for conducting PoAP [5-7] and so also the variation of CV profiles and movements of redox peaks, within the potential interval, -0.4 / +1.0 V vs Ag/AgCl with cycling.

Differently from the previous electro-synthesis in neutral media, the conducting nature of PoAP in acidic media is here confirmed by the continuous variation of anodic and cathodic currents, registered with cycling, indicative of a continuous film growth. The so different voltammetric profiles are certainly depending on the electrolyte solution employed for the electrosynthesis and clearly confirms the literature [5-7] reports on oAP polymerization routes tunable with pH.

In our case the process was stopped after 125 cycles (i.e. after about one hour and a half) when the pair of redox peaks, attributable to the process of oxidation and reduction of the polymer, was clearly evident. This is better shown in the figure inset where the CV of the deposited film in perchlorate electrolyte (deprived of oAP monomer) is reported in the shorter potential range that just includes the polymer redox peaks. Such peaks are lost when the conducting film is cycled in neutral media (data not shown) thus indicating that proton doping is responsible for the redox process and for maintaining the film electro-activity.

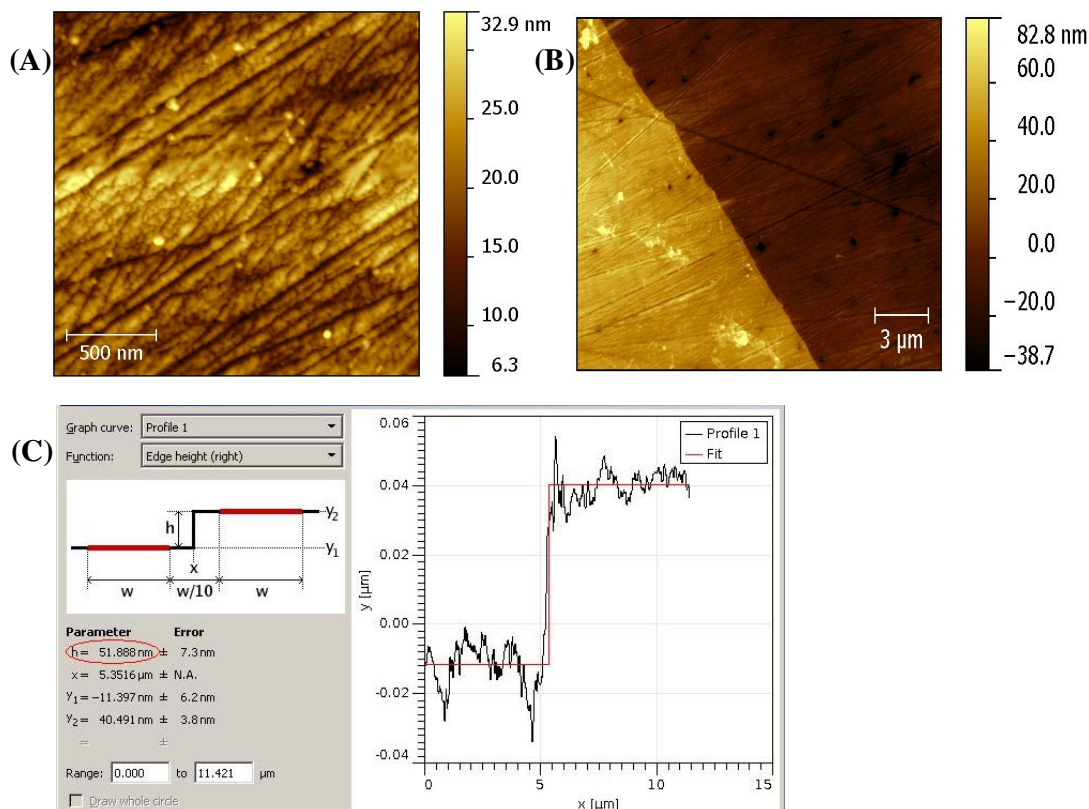


Figure 7. AFM images of the conducting PoAP film (A) and of the Pt/PoAP border region (B) with estimation of the polymer thickness (C).

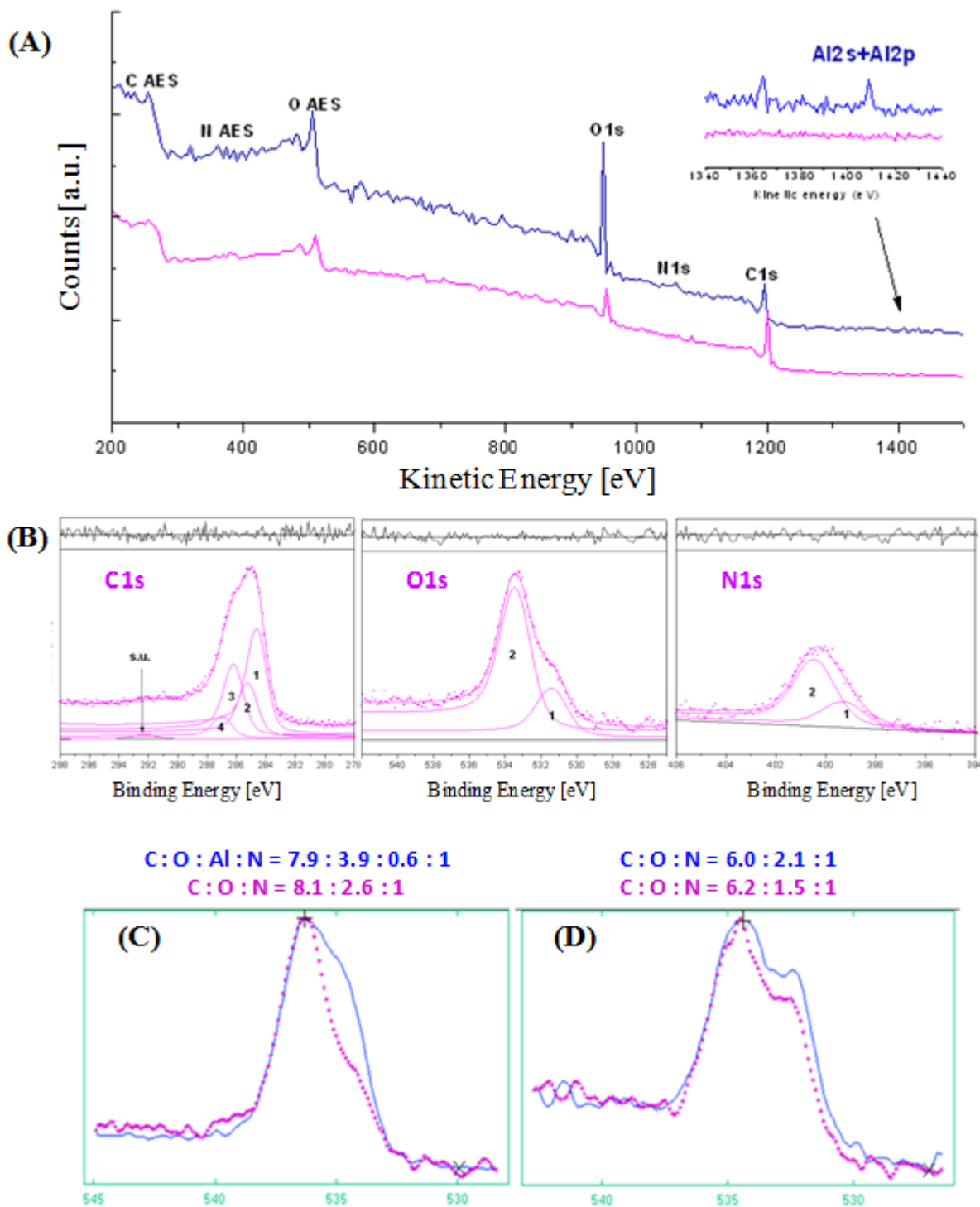


Figure 8. XPS wide spectra of conducting PoAP films with the presence (blue) and absence (purple) of alumina contamination (A); curve-fitted C1s, O1s and N1s regions, acquired from purple spectra (B). Spectra difference of O1s regions, before and after removal of alumina, for conducting (C) and insulating (D) films.

Figures 7 and 8 show, respectively, AFM images and XPS analysis of conducting PoAP acquired in the reduced state (potential scan ended at -0.2 V vs Ag/AgCl) for a better comparison with insulating PoAP.

AFM images confirm the characteristics of PoAP film grown onto blank 1 substrates, at any magnification, (7A-B). In addition, the film thickness could also be estimated by elaborating the 7B image at the border (here well recognisable) between deposited film and blank substrate: the measurement reported in 7C for the reduced PoAP gives a thickness of 52 ± 7 nm, also confirmed for the oxidized state (not shown) thus further proving the film homogeneity.

The parallel XPS analyses have highlighted instead an unexpected problem related to the cleaning of the platinum, blank 1, substrates. As shown in the blue labeled wide spectrum of Figures 8A, aluminum was detected as an additional element, most likely derived from the remains of the abrasive alumina used for the substrates cleaning.

This fact, has raised a number of considerations:

- based on reference spectra registered in our laboratory and literature data [18,28], oxygen signals from alumina fall in the same energy range of the acquired O1s regions while Al2p and Al2s peaks fall in the same energy range of Platinum 4f region;
- in the case of insulating PoAP, aluminum was probably present but completely masked by the platinum 4f signals, quite intense, given the thinness of the over layer film and its higher sensitivity factor [15-17]. If so, the oxygen enrichment, and particularly the O1 component, could partly be due to alumina contamination;
- in the case of conducting PoAP, the underneath platinum is not detected at all, accordingly to the thickness estimated by AFM, much above the XPS analytical depth [16,18], therefore aluminum can be registered without platinum interference. However, the presence of aluminum in the outer layers of the polymers detected by XPS signifies that it has been displaced by the platinum surface during polymerization, as happened with oxygen, and, most likely, with any preexisting contamination.

To settle these issues, the cleaning procedure for platinum blank 1 substrate has been revised and film deposition of conducting PoAP repeated. Once the absence of aluminum was confirmed by XPS, see the purple wide spectrum in Figures 8A, the new cleaning procedure (*vide infra*) was thereafter adopted for the completion of PoAP characterization with combined spectroscopic analyses.

3.4 Combined spectroscopic analyses of insulating and conducting PoAP

The information provided so far could, perhaps, be considered trivial if not aware of the many steps necessary to complete any given experiment each subjected to procedural errors adding to the final results.

Here we have repeated experiments and also tried to individuate systematic errors that would affect accuracy, either related to each analytical procedure and to the samples storage and their transfer to ex-situ analyses.

Regarding the improvement of the cleaning procedure reported in Experimental, to remove any alumina residues from platinum surfaces, it was found necessary to reverse points 1 and 2 therein listed, i.e. the mechanical cleaning by alumina was followed by the chemical etching in nitric acid. The

efficacy of the revised procedure is shown in the inset of Figures 8A: no signals are detectable in the 'purple' partial wide, enlarged just around the energy window of Al signals.

The note on cleaning added in Experimental should then be reminded whenever appropriate, considering that adsorption on platinum surfaces of any kind seems not to be identifiable in the voltammograms when dealing with oxidation and adsorbed contamination at the sub-nanometers level, as in our conditions [25].

Changes in composition before and after the 'complete' removal of alumina are compared in Figures 8C (conducting PoAP) and D (insulating PoAP) where attention is focused on both O1s regions, the most affected among the polymers detailed regions.

Notwithstanding the abatement of the total O1s intensity after removal of overlapping oxygen due to alumina residues, the relative C:O:N ratios, taking nitrogen as the reference element for both polymers, show the partial O/N ratios exceeding unity. The excess oxygen is more relevant for conducting PoAP that additionally shows, at difference of insulating PoAP, the partial C/N ratio exceeding that expected by the 'repeat' of the monomer formula (C:O:N = 6:1:1) as already said.

Preliminary curve-fitting of detailed regions for the 'aluminum-cleaned' conducting PoAP (Figure 8B) anticipate the presence of carbonyl-type peaks in the carbon regions that correlate with O1 peaks and of water (adding to O2 peaks) strongly adsorbed along PoAP chains, likely through H-bonds, that would justify oxygen in excess, as found for oAP monomer and, previously, for other studied polymers [19, 29-31].

The curve-fitted C1s, O1s, N1s regions of insulating PoAP (not shown) show exactly the same 'resolved' chemical states as for the conducting PoAP. Their spectral similarity includes also surplus oxygen adding to O2 peak and co-presence of O1 and C4 peaks (carbonyl-type signals in both carbon- and oxygen- 1s regions). However, as it can be observed in Figure 8D the mentioned difference of O1s spectra are not so relevant for insulating PoAP as if contributions, other than carbonyl-type groups, add to it. Considering that, in this case, the XPS analytical depth may include the entire PoAP film plus substrate layers, it is reasonable to think of signals from oxidized platinum, adding to O1 [25, 26].

Whether oxidized groups are just those terminating and/or initiating the conducting and insulating chains and if hydrating water mainly permeates the outer 10 nm layers, detectable by XPS, rendering similar 'views' of both insulating and conducting PoAP, it can only be proved by repeating XPS at different experimental conditions (work in progress, vide infra) and by the help of complementary spectroscopy having different analytical depths, as Raman spectroscopy discussed in the next paragraph.

3.5 Micro-Raman Spectroscopy

Raman spectra are reported in Figures 9 and concern oAP monomer (9A), conducting polymer thick about 52 nm (9B) and random aggregates protruding over the film deposited (9C), as seen by AFM.

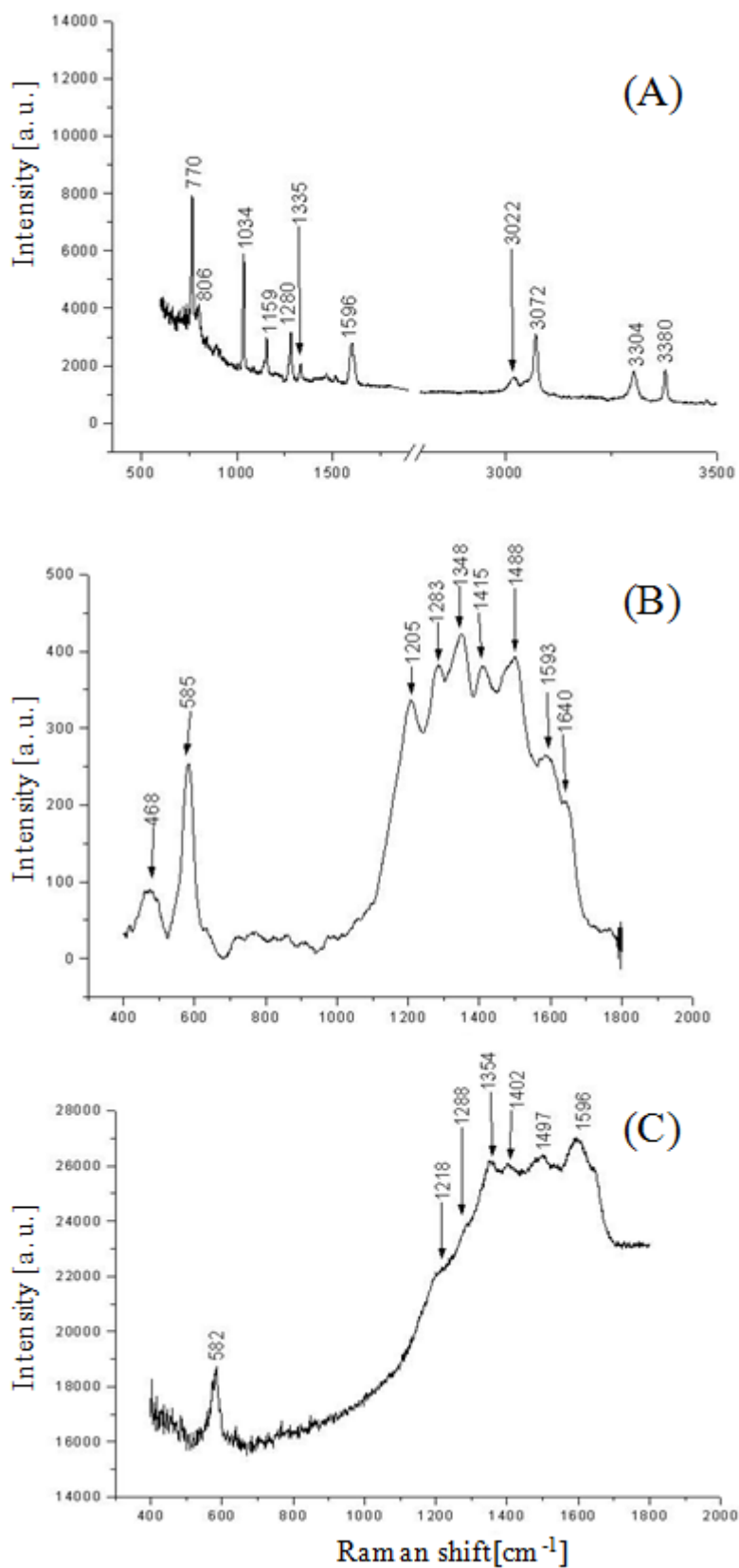


Figure 9. Raman spectra of (A) oAP crystals; (B) conducting PoAP deposited onto blank 1 substrate and (C) aggregates protruding over the deposited film.

The spectrum acquisition of insulating PoAP was unsuccessful. Given the small film thickness, clearly not suited to Raman detection, no characteristic signals could be distinguished above an amorphous, unspecified, background (not shown). Since the XPS results can quite compensate for the lack of information from Raman, as already evidenced in the previous paragraphs, the resort to an alternative technique was not considered necessary for the moment.

Differently, the Raman spectra, 9B-C, of conducting PoAP could be acquired and studied in comparison with that of oAP monomer, 9A, and literature. Some common features are seen in PoAP and oAP spectra while new features specific to PoAP are indicative of the polymerization that has occurred, as already confirmed by literature data [32-34]. Most interesting is the similarity in 9B and 9C of peaks Raman shifts. This means that aggregates are of the same matter as PoAP or, at least, that the laser beam focused on aggregates, to allow comparison, has not provided new vibrational modes.

Taking into account parallel UV analyses performed in situ [35] and ex-situ [36], relatively to conducting PoAP, experimental results seem to converge on the idea that oligomers may form with different conjugation lengths, from common 'soluble intermediates', and aggregate onto the electrode surface under the effect of progressive potential scans concomitantly to oAP polymerization.

The PoAP (and aggregates) assignments from Raman spectra are reported in Table 2 and agree with literature [5-7, 32-36] and mostly with XPS findings, as derived by the curve-fitted regions reported in Figure 8B.

Table 2. Vibrational bands assigned to Raman spectra ($\lambda_0 = 632.8$ nm) of conducting POAP in Figure 9B.

Band position (cm ⁻¹)	Assignment
468	C-C bending out of plane of the aromatic rings
585	Ring deformation of the benzenoid units
1205	C-H bending in plane + C-C stretching
1283	C-N stretching + C-O stretching
1348	C-N ⁺ stretching
1415	C-C stretching of quinoid ring + C-N ⁺ stretching of radical
1488	semiquinone
1593	C=N stretching of quinoid units
1640	C=C stretching of quinoid units + NH bending in plane of secondary amines
	C=N stretching

The aromatic C-C carbons (C1 plus shake up), amine and imine groups (C2, C3, N1, N2) and ether like C-O groups (C3, O2) are confirmed by both XPS [21, 37] and Raman spectroscopies. But the oxidized groups of carbonyl-types (C4, O1) are not 'seen' by Raman and we should from this consider the instrumental specificities of both techniques [38]: XPS as a surface-specific technique provides an averaged composition of a large surface area (mm) within a vertical depth of around ten

nanometres whereas Raman spectroscopy provides information from smaller spots at deeper sampling depths (sub-micron volumes).

Oxidized groups and oxygen surplus may be the results of ‘surface-related effects’, thus only detectable by XPS, arising from the sudden off-polarization (CV scans, ending potentials) and post-synthesis rinsing (ultra-pure flowing water plus drying gaseous nitrogen) of the treated platinum before ex-situ analyses [37].

4. CONCLUSIONS

This work has given the basis and clarified the experimental paths for the electrosynthesis and characterization of PoAP films deposited on platinum substrates at acidic and neutral pH.

The results here obtained have provided information on the starting monomer (oAP), platinum substrates as well as on the electrodeposited polymers and their inner (Pt) and outer (environments) interfaces.

Indeed, light was shed upon the necessity of using different analytical techniques for investigating complex, layered systems as ours under study. In particular, evidences were given of the correlation between topography/ morphology of blank substrates and deposited polymers by high-definition AFM images and chemical composition by spectroscopy and of the manner in which XPS and Raman complement each other.

XPS is paramount in providing chemical analysis of nanoscale surfaces. In our case, the XPS depth of analysis included the entire thickness of insulating PoAP and its inner interface with platinum while it maximized the outer layers and outer interface of the thicker conducting PoAP. Nevertheless, a strong similarity in composition was seen for both polymers, substantiated by the “common” presence of carbonyl-type groups and oxygen in excess, most likely due to strongly entrapped water.

The different relative intensities of the same chemical groups and their rationale in PoAP formation at different pH seem the basic keys to understanding the real nature of their conducting and insulating states.

To this aim, following the CV profiles, comparative analyses will be continued by changing the number of growth cycles to complete in-depth studies of both polymers. In perspectives, the design of switchable electrochemical devices, depending on PoAP conductive/insulating states, will be considered also in view of possible bio-application.

ACKNOWLEDGEMENTS

The authors thank Dr. Fausto Langerame for XPS assistance, Dr. Neluta Ibris (CIGAS) for AFM acquisitions and Dr. Angela DeBonis for Raman spectra. Antonio Guerrieri and Rosanna Ciriello acknowledge the financial support by MIUR (PRIN 2009).

References

1. L. Sabbatini, C. Malitesta, E. De Giglio, I. Losito, L. Torsi, P.G. Zambonin, *J. Electron Spectrosc. Relat. Phenom.* 100 (1999) 35-53.
2. S. Biallozor, A. Kupniewska, *Synth. Met.* 155 (2005) 443-449.

3. H.J. Salavagione, J. Arias, P. Garcés, E. Morallón, C. Barbero, J.L. Vázquez, *J. Electroanal. Chem.* 565 (2004) 375-383.
4. C. Barbero, J.J. Silber, L. Sereno, *J. Electroanal. Chem. Interfacial Electrochem.* 263 (1989) 333-352.
5. R. Tucceri, P.M. Arnal, A. Scian, *ISRN Polymer Sci.* (2012).
6. R. Tucceri, P.M. Arnal, A.N. Scian, *J. Spectrosc.* (2013).
7. R. Tucceri, P.M. Arnal, A.N. Scian, *Can. J. Chem.* 91 (2013) 91-112.
8. J. E. Castle, A.M. Salvi, *J. Electron Spectrosc. Relat. Phenom.* 114 (2001) 1103-1113.
9. P. Lang, Z. Mekhalif, B. Rat, F. Garnier, *J. Electroanal. Chem.* 441 (1998) 83-93.
10. Y. Yang, Z. Lin, *Synth. Met.* 78 (1996) 111-115.
11. J. M. Ortega, *Thin Solid Films* 371 (2000) 28-35.
12. R. Ciriello, T.R.I. Cataldi, D. Centonze, A. Guerrieri, *Electroanal.* 12 (2000) 825-830.
13. D.A. Shirley, *Phys. Rev. B: Solid St.* 5 (1972) 4709-4714.
14. J.E. Castle, H. Chapman-Kpodo, A. Proctor, A.M. Salvi, *J. Electron Spectrosc. Relat. Phenom.* 106 (2000) 65-80.
15. C.D. Wagner, L.E. Davis, M.V. Zeller, J.A. Taylor, R.M. Raymond, L.H. Gale, *Surf. Interface Anal.* 3 (1981) 211-225.
16. D. Briggs, M.P. Seah, *Practical surface analysis*, second ed., Wiley, Chichester, 1990.
17. M.P. Seah, D. Briggs, J.T. Grant, *Surface analysis by auger and X-ray photoelectron spectroscopy*, IM Publications and Surface Spectra, Chichester, 2003.
18. NIST database. <http://www.nist.gov/srd/surface.htm> (last accessed 2013)
19. R. Ciriello, A. Guerrieri, F. Pavese, A.M. Salvi, *Anal. Bioanal. Chem.* 392 (2008) 913-926.
20. G.E. De Benedetto, C. Malitesta, F. Palmisano, P.G. Zambonin, *Anal. Chim. Acta* 389 (1999) 197-204.
21. G. Beamson, D. Briggs, *High resolution XPS of organic polymers*. The Scienta ESCA300 Database, Wiley, Chichester, 1992.
22. S.N. Kumar, G. Bouyssoux, F. Gaillard, *Surf. Interface Anal.* 15 (1990) 531-536.
23. S. Mu, *Synth. Met.* 143 (2004) 259-268.
24. A. Guerrieri, R. Ciriello, D. Centonze, *Biosens. Bioelectron.* 24 (2009) 1550-1556.
25. M. Peuckert, F.P. Coenen, H.P. Bonzel, *Electrochim. Acta* 29 (1984) 1305-1314.
26. C.C. Hu, K.Y. Liu, *Electrochim. Acta* 44 (1999) 2727-2738.
27. T. Laiho, J.A. Leiro, *Appl. Surf. Sci.* 252 (2006) 6304-6312.
28. C.D. Wagner, W.M. Riggs, L.E. Davis, J.F. Moulder, G.E. Muilenberg, *Handbook of X-Ray Photoelectron Spectroscopy*, first ed., Perkin Elmer, Eden Prairie, 1979.
29. A.M. Salvi, P. Moscarelli, B. Bochicchio, G. Lanza, J.E. Castle, *Biopolymers* 99 (2013) 292-313.
30. J.E. Castle, A.M. Salvi, R. Flaminia, G. Satriano, *Surf. Interface Anal.* 44 (2012) 246-257.
31. A.M. Salvi, P. Moscarelli, G. Satriano, B. Bochicchio, J.E. Castle, *Biopolymers* 95 (2001) 702-721.
32. B. Palys, M. Marzec, J. Rogalski, *Bioelectrochemistry* 80, (2010) 43-48.
33. A.A. Shah, R. Holze, *J. Electroanal. Chem.* 597 (2006) 95-102.
34. H.J. Salavagione, J. Arias-Pardilla, J.M. Pérez, J.L. Vázquez, E. Morallón, M.C. Miras, C. Barbero, *J. Electroanal. Chem.* 576 (2005) 139-145.
35. D. Gonçalves, R.C. Faria, M. Yonashiro, L.O.S. Bulhões, *J. Electroanal. Chem.* 487 (2000) 90-99.
36. F. Armijo, L.I. Canales, R. Del Rio, M.A. Del Valle, *J. Chil. Chem. Soc.* 54 (2009) 158-162.
37. I. Losito, C. Malitesta, I. De Bari, C.D. Calvano, *Thin Solid Films* 473 (2005) 104-113.
38. A. Macchia, M.L. Tabasso, A.M. Salvi, M.P. Sammartino, S. Mangialardo, P. Dore, P. Postorino, *Surf. Interface Anal.* 45 (2013) 1073-1080.